Proceedings of Machine Learning Research vol 242:1–11, 2024

Towards Bio-Inspired Control of Aerial Vehicle: Distributed Aerodynamic Parameters for State Prediction

Yikang Wang YIKANG.WANG@CRANFIELD.AC.UK
Adolfo Perrusquia ADOLFO.PERRUSQUIA-GUZMAN@CRANFIELD.AC.UK
Dmitry Ignatyev D.IGNATYEV@CRANFIELD.AC.UK
School of Aerospace, Transport and Manufacturing, Cranfield University, UK

Abstract

In an era where traditional flight control systems are increasingly strained by the demands of modern aerial missions, this research introduces a novel integration of bio-inspired sensing mechanisms into aerial vehicle control systems, aimed at revolutionizing the adaptability and efficiency of UAV operations. Current gust suppression technologies often activate only after disturbances have occurred, highlighting significant limitations in real-time responsiveness and computational efficiency. With a specific emphasis on employing distributed aerodynamic parameters for predicting flight states, the study utilizes a Convolutional Neural Network (CNN) and a Long Short-Term Memory (LSTM) network to investigate the predictive capabilities of these models under varying conditions, including scenarios with full and limited input data. The models were assessed on their ability to forecast the pitch rate of Unmanned Aerial Vehicles (UAVs), examining both the precision of predictions in response to different historical input sizes and their robustness against simulated sensor noise. Results highlight the potential of using aerodynamic data to enhance the reliability and adaptability of flight control systems, significantly reducing dependency on specific sensor inputs. This approach not only demonstrates the effectiveness of integrating sophisticated machine learning models with aerospace technology but also paves the way for more adaptive, efficient control systems in UAV operations.

Keywords: Bio-inspired sensing, Aerodynamic parameters, Flight state prediction, Convolutional Neural Networks, UAV, Aerospace engineering

1. Introduction

Aerospace engineering currently faces significant challenges in flight control systems, particularly with autonomous gust suppression technologies. Traditional control systems, despite their critical role in various flight tasks, show marked deficiencies in handling gust disturbances. Historically, gust response has depended on pilots or autopilots initiating corrective actions after disturbances have occurred. However, these reactionary measures, often delayed, can jeopardize mission success, especially under strict altitude constraints. Binias et al. (2020)

Although autopilot systems employing classical control theories have used traditional control surfaces equipped with strain gauges to feedback, achieving only a 50% improvement in gust load and flight ride quality, these enhancements do not meet the demands of modern aerial missions. Regan and Jutte (2012) In recent years, the development of advanced sensing technologies, particularly the introduction of Doppler Light Detection and Ranging (LIDAR) systems, has made it possible to anticipate incoming gusts, thereby enhancing gust response effectiveness to 80%. Hamada et al. (2019) Nonetheless, the practical implementation of preview control is significantly constrained by several factors: the accuracy and real-time availability of gust information, as well as the computational power and weight limitations associated with LIDAR systems. Khalil and Fezans (2019)

These challenges highlight the need for more advanced solutions to enhance the reliability and efficiency of gust suppression technology in both manned and unmanned aviation tasks.

One emerging solution to these challenges is the adoption of bio-inspired sensing mechanisms. The natural world, through evolutionary processes, has endowed creatures such as birds, insects, and bats with exceptional flight capabilities and sophisticated sensing mechanisms.Brown and Fedde (1993) For instance, bats utilize fine hairs on their wings to detect changes in airflow, guiding their flight manoeuvres with remarkable agility and precision.Sterbing-D'Angelo et al. (2011) These capabilities enable them to navigate complex environments effectively. Recent research developments have focused on the 'Fly-by-Feel' paradigm Kopsaftopoulos et al. (2015), which emphasizes real-time, high-resolution state-sensing and self-diagnostic functionalities in aircraftKopsaftopoulos et al. (2016). A significant advance in this area has been led by Stanford University, which has integrated bio-inspired sensor networks into UAV wings Chen et al. (2018). These networks, comprising piezoelectric sensors, strain gauges, and temperature detectors, significantly enhance the sensory capabilities of aircraft, marking a substantial leap in aviation sensor technology Kopsaftopoulos et al. (2018)Chen et al. (2019).

As sensor arrays and computational models become increasingly complex, they do not only add weight but also challenge the real-time delivery of predictive information crucial for autonomous gust suppression control systems. In response, this study explores the feasibility of using aerodynamic data, such as air pressure data on wings, for predictive analysis. This approach offers a new dimension in flight control, utilizing simulation data to assess the integration of bio-inspired sensing principles into various aerial vehicles' control systems. While this study does not involve the direct application of air pressure sensors on wings, it investigates this concept through simulated scenarios. The focus is to determine whether bio-inspired sensing, as indicated by the simulated data, can enhance the manoeuvrability, responsiveness, and safety of a range of aerial vehicles. This method aims to bridge the gap between biological insights and aerospace technology, replicating the adaptability and efficiency observed in natural flyers. The goal is to establish a foundation for future designs of aerial vehicles that incorporate bio-inspired sensing capabilities, thereby propelling the field of aerospace engineering towards more adaptive and intelligent flight systems.

The remainder of this paper is organized as follows. Section 2, *Method*, describes the simulation setup and the machine learning models used for the study, detailing the data generation, the specifics of the 1D Convolutional Neural Network (CNN), and the Long Short-Term Memory (LSTM) network implementations. It also outlines the experimental conditions under which the models were evaluated, including scenarios with different historical input sizes and noise levels. Section 3, *Results*, presents the findings from the experiments, discussing the models' performance in terms of Mean Squared Error, Maximum Error Percentage, and Prediction Time under optimal and limited input conditions. This section also explores the impact of noise on the predictive accuracy and reliability of the models. Finally, Section 4, *Conclusion*, synthesizes the insights gained from the research, discusses the implications for real-world applications, and suggests directions for future research.

2. Method

This study investigates the feasibility of using distributed airflow data collected from aircraft wings to predict future flight states of unmanned aerial vehicles (UAVs). To facilitate this investigation, we generate a comprehensive dataset through simulation methods, tailored specifically for training ad-

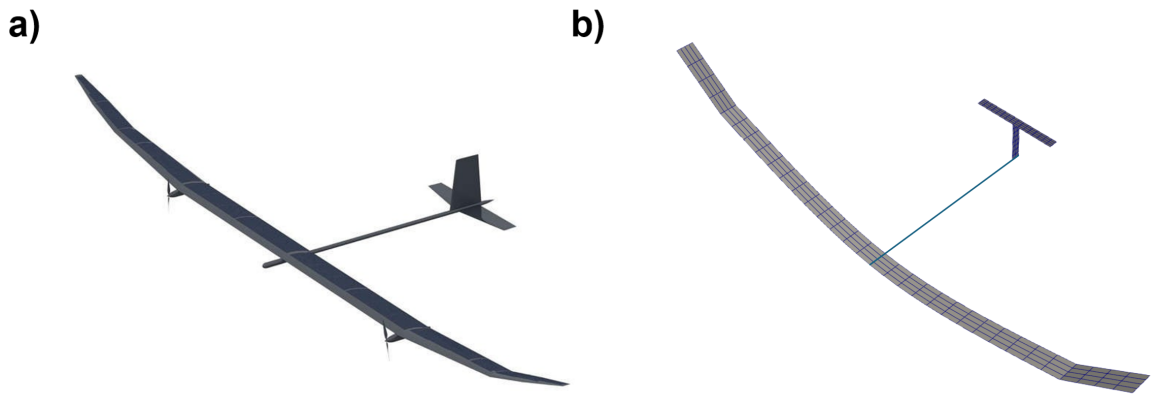

Figure 1: Comparison of the PHASA-35 UAV and the simplified HALE model used in the research. Part (a) of the figure features the PHASA-35 developed by BAE Systems, an example of HALE unmanned aircraft. It is designed to provide persistent and cost-effective imagery and communications.BAE (2023) Part (b) of the figure depicts the simplified HALE model utilized in this research, tailored specifically to study the dynamics of airflow and state prediction in UAV systems.

vanced machine learning models. The dataset feeds into two primary models: the 1D Convolutional Neural Network (1D CNN) and the Long Short-Term Memory (LSTM) network, both renowned for their robust performance in time-series prediction tasks. These models are chosen to analyze aerodynamic data due to their proven effectiveness in similar predictive scenarios.

Detailed descriptions of the training data generation process and the application of these models are provided in the subsequent sections, outlining each step from data simulation to model evaluation.

2.1. Experiment setup

In this study, we use SHARPy (Simulation of High Aspect Ratio aeroplanes in Python) del Carre et al. (2023), a tool specifically designed for simulating aircraft with high aspect ratio wings, such as the structurally simplified T-Tail High Altitude Long Endurance (HALE) model employed in our simulations (see Figure 1). The selection of the HALE model is particularly apt for two key reasons. First, due to its lightweight and highly flexible structure, the HALE aircraft is inherently more sensitive to gust influences, making it an ideal candidate for studying dynamic aerodynamic responses. Second, HALE aircraft are required to maintain flight stability and consistent altitude during long-duration missions, aligning precisely with the objectives of this research which aims on enhancing gust suppression capabilities. As shown in Figure 1, the wing consists of a total of 128 panels, each providing crucial aerodynamic data from the simulation. This panel information is used to simulate distributed aerodynamic parameters, similar to what would be captured by a real-world sensor array. In this study, we did not address the optimization and selection of sensor array positions; therefore, data from all wing panels were used to obtain the most comprehensive aerodynamic parameter inputs.

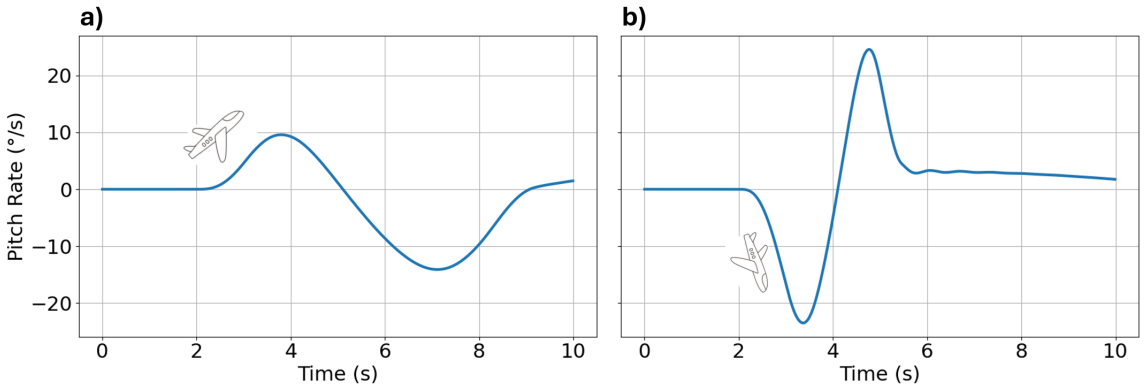

Figure 2: Examples of the "1-cosine" gust profiles used in the study. (a) represents a mild up-gust and (b) represents a more severe down-gust.

We conducted simulations across 300 different gust scenarios, each characterized by unique intensity and duration, to simulate a diverse range of gust conditions and test the model's real-world predictive performance. These scenarios included both up-gusts and down-gusts, employing a "1-cosine" gust shape. This particular gust profile is commonly used in aeronautics for testing aircraft resilience and dynamic response under transient conditions. The "1-cosine" gust effectively models a sudden drop in wind speed followed by a gradual recovery, which simulates real-world gust encounters that a UAV might face during flight (see Figure 2). For the aerodynamic simulations, we utilized the 'StaticUvlm' solver within SHARPy, configured with 224 bound panels and 1120 wake panels. This setup ensures an accurate representation of the UAV's aerodynamic behavior under various flight conditions.

The data collected from these simulations includes the UAV's pitch rate changes over a period of 10 seconds, as well as the circulation and rate of change of circulation on the wing panels. We recorded these data with a high-resolution time step of 0.01 seconds, resulting in 1000 time nodes per data segment. This high granularity allows for a detailed analysis of the UAV's aerodynamic responses to gusts, providing insights into the dynamics and stability of the aircraft under such conditions.

2.2. Feasibility of Predicting Flight States Using Aerodynamic Data

The first phase of the experiment is designed to investigate the influence of various historical input sizes on the model's predictive performance using aerodynamic data collected from UAV wings. This involves adjusting the historical window size i, analyzing its impact on model accuracy and computational efficiency. As part of the aerodynamic data, **circulation**, denoted as Γ, refers to the integral of the velocity field along a closed loop encompassing the wing. It is a fundamental parameter used to quantify the rotational motion of air around the wing, which in turn affects the lift generated by the wing. Understanding and predicting changes in circulation are crucial for accurate flight state predictions in dynamic environments.

Once the optimal input size is identified, the dataset is augmented with Gaussian noise to simulate real-world sensor inaccuracies and test the robustness of the models under these conditions.

The noise is added using the formula:

$$\text{Noise} = \sigma \cdot \epsilon \tag{1}$$

where σ is tailored as a percentage of the data's range to mimic realistic measurement errors, and ϵ is sourced from a standard normal distribution.

The goal of this stage is to utilize this optimally configured noisy data to predict the pitch rate at a future time step $t + k \cdot T$, where $k = 25$ and $T = 0.01s$. This short prediction horizon is selected based on the real-time operational requirements and the high time-sensitivity of aerodynamic data, allowing UAV flight control systems to respond quickly to dynamic changes in the environment—key for maintaining stability and ensuring safety.

The mathematical representation for this prediction model is:

$$q_{t+k\cdot T} = f(q_{t-i:t}, \Gamma_{t-i:t}) \tag{2}$$

where f signifies the predictive model function, t is the current time step, $t - i$ indicates the start of the time window incorporating i historical data points, and t is the end of the time window.

2.3. Predicting Flight States Under Limited Input Conditions

Following the optimization of input data and the introduction of noise, the second experiment assesses the model's performance under limited input conditions. Here, historical pitch rate data is excluded, and only circulation (Γ) is used as input. This scenario simulates potential failures or unavailability of conventional flight sensors and examines the resilience of the model when deprived of comprehensive data inputs.

The function for this constrained input model is simplified to:

$$q_{t+k\cdot T} = f(\Gamma_{t-i:t}) \tag{3}$$

This test evaluates the model's capability to predict flight states using minimal aerodynamic data, emphasizing the model's adaptiveness and robustness in handling gusty conditions and its potential to develop accurate predictive capabilities even in adverse operational environments.

Each phase of the experiments is meticulously designed to progressively evaluate the potential of aerodynamic data in enhancing the predictiveness and reliability of flight control systems under diverse and challenging conditions.

2.4. 1D Convolutional Neural Networks (1D CNNs)

1D Convolutional Neural Networks (1D CNNs) are designed for analyzing sequential data such as time-series. Unlike 2D CNNs used in image processing, 1D CNNs apply convolution operations across time to capture temporal patterns.

As shown in Figure 3, the CNN model in this study starts with two convolutional layers, each with 128 filters and a kernel size of 3, designed to capture temporal patterns from the sequential input data. This is followed by a flattening layer that transforms the 2D output of the convolutions into a 1D array, which then passes through two more dense layers with 512 units each. The model culminates in a single-unit output layer, designed to predict the continuous target variable. The model is compiled with the Adam optimizer and uses mean squared error as the loss function, emphasizing the model's focus on minimizing the prediction error during training.

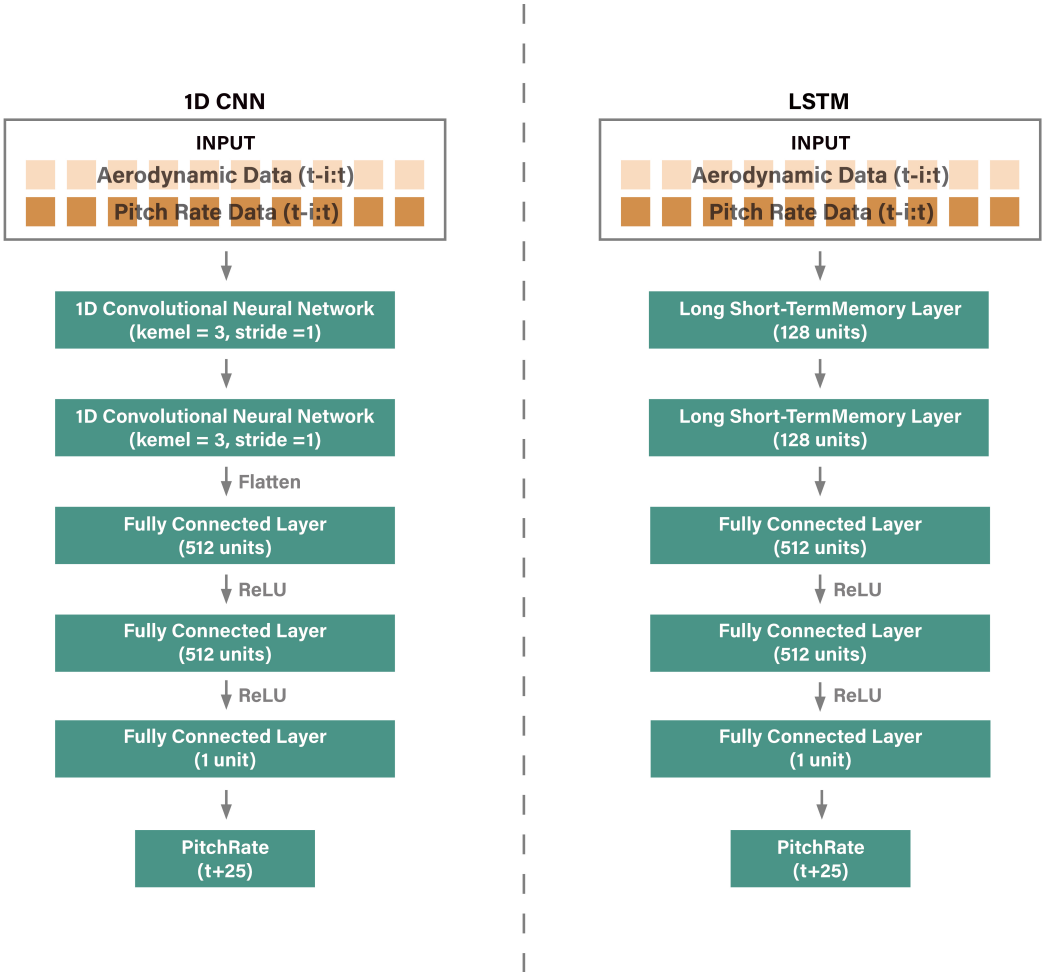

Figure 3: Illustration of the predictive modeling architecture used in this study.

2.5. Long Short-Term Memory Networks (LSTMs)

LSTMs are a type of recurrent neural network designed to avoid long-term dependency problems in standard RNNs. They manage information flow through three distinct gates: the Forget Gate, the Input Gate, and the Output Gate. These gates enable LSTMs to make informed decisions about which information to store, discard, and output at each time step, making them effective for modeling time series data.

The LSTM model in this study features two LSTM layers with 128 units each, where the second LSTM layer operates without return sequences to compact the data into a more dense form (see Figure 3). This is followed by two dense layers, each with 512 units, using 'relu' activation to introduce non-linearity and facilitate feature learning at a higher abstraction level. The model culminates in a single-unit output layer, designed to predict the continuous target variable.

3. Results

This section presents the experimental outcomes obtained from the 1D CNN model and LSTM model, developed for the prediction of flight states. The performance of the model is evaluated using three metrics: Mean Squared Error (MSE), Maximum Percentage Error, and Prediction Time. These metrics provide insight into each model's accuracy, reliability, and efficiency under different configurations.

The MSE is a standard metric in regression analysis, calculated as the average of the squared differences between the predicted values and the actual values. It is a measure of the quality of an estimator—it is always non-negative, and values closer to zero are better. The MSE formula is expressed as:

$$MSE = \frac{1}{n}\sum_{i=1}^{n}(Y_i - \hat{Y}_i)^2 \tag{4}$$

In this equation, n denotes the number of samples, Y_i represents the actual value, and $\hat{Y}_i$ signifies the predicted value.

The Maximum Error Percentage is introduced as an additional metric to assess the performance of the model with respect to the most significant deviations in the predicted values from the actual values, relative to the range of pitch values observed in the test dataset. This metric provides insight into the worst-case error scenario, which is crucial for evaluating the robustness of the model in practical applications. The MEP is calculated as:

$$MEP = \left(\frac{\max(|Y_i - \hat{Y}_i|)}{\max(Y_i) - \min(Y_i)}\right) \times 100\% \tag{5}$$

Here, $\max(|Y_i - \hat{Y}_i|)$ represents the maximum absolute error across all predictions, while $\max(Y_i) - \min(Y_i)$ denotes the range of the actual pitch values in the dataset. Expressing this ratio as a percentage provides a scale-independent metric that can be easily interpreted and compared across different models or experimental setups.

The MSE provides a broad measure of the model's accuracy across all predictions, while the MEP offers a focused view of the model's performance in handling the most extreme discrepancies between the predicted and actual values. By evaluating both metrics, we gain a comprehensive understanding of the model's effectiveness and areas where improvements may be necessary, particularly in ensuring the model's reliability under various operational conditions.

3.1. Model Performance Under Optimal Input Conditions

The LSTM model shows a trend of decreasing MSE as the historical window size increases, with the lowest MSE recorded at i=13 (0.1132), see Figure 4. This improvement indicates that the LSTM model efficiently utilizes longer data sequences to enhance prediction accuracy, particularly beneficial in dynamic environments such as UAV flight control. The MEP exhibits relatively stable behavior, slightly increasing at larger window sizes, suggesting consistent model performance across varying inputs. Prediction times show slight increases with larger data inputs, which is expected due to the additional computational demands of processing more extensive sequences. The fluctuation in prediction time observed at i=17 may be attributed to performance variations in the computer used during the execution of the model.

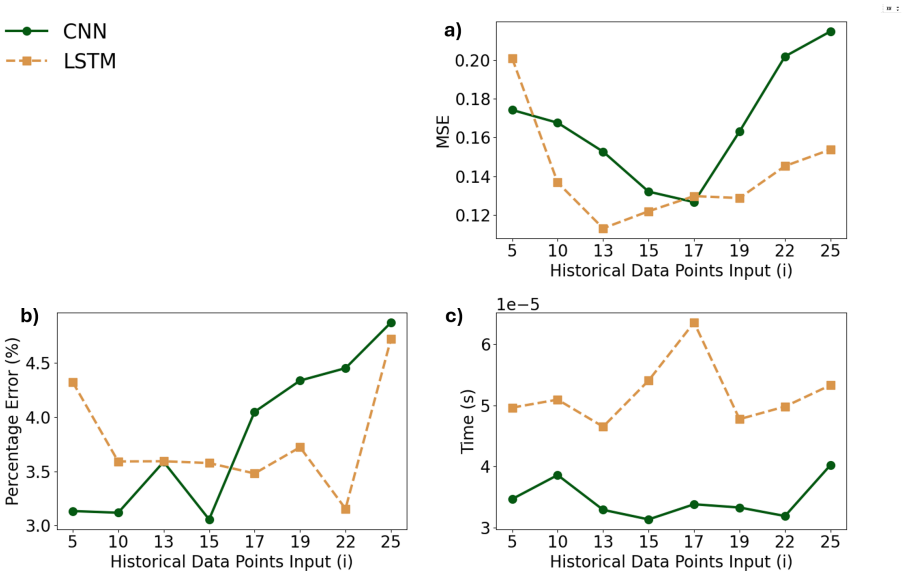

Figure 4: Performance metrics of 1D CNN and LSTM models across varying historical window sizes i. a) Overall MSE: Charts the MSE for both models, highlighting an initial decrease followed by an increase in error as the historical window size continues to expand. b) MEP: Illustrates the peak error percentages for each model across the window sizes, showing variability in error response as window size changes. c) Average Prediction Time per Timestep: Depicts the prediction time for each model at different window sizes, reflecting their processing efficiency and computational demand. The prediction times for both models are negligible compared to the 0.25-second prediction horizon, achieving near real-time prediction. The tests were conducted on a system equipped with an AMD 3900X CPU, a NVIDIA 2080 Super GPU, and 32GB of RAM.

The CNN model displays optimal performance at i=17 with an MSE of 0.1267, indicating a sweet spot where the model balances accuracy and overfitting risks effectively (see Figure 4). Beyond this point, both MSE and MEP increase notably, particularly at i=25 (MSE=0.2147, MEP=4.8758), pointing towards overfitting issues as the model becomes overly tuned to the training data. This is evident from the significant spikes in error metrics at higher window sizes. Despite this, CNN maintains relatively lower prediction times across all inputs, which may be crucial for applications requiring rapid data processing.

Transitioning to noise impact testing, it was decided to utilize the input sizes that previously demonstrated the best performance for each respective model in the presence of noise. Thus, the CNN model was tested further at i=17 and the LSTM model at i=13, providing a basis to assess how each model copes with additional data complexities introduced by noise. This strategic choice aims to discern the robustness of each model under realistic operational conditions where data accuracy might be compromised.

For the CNN model, increasing noise levels resulted in substantial elevations in MEP and MSE, with MEP rising dramatically to 6.6483 at 20% noise level (see Figure 5). This significant increase underscores the CNN's sensitivity to noisy conditions, potentially limiting its deployment in en-

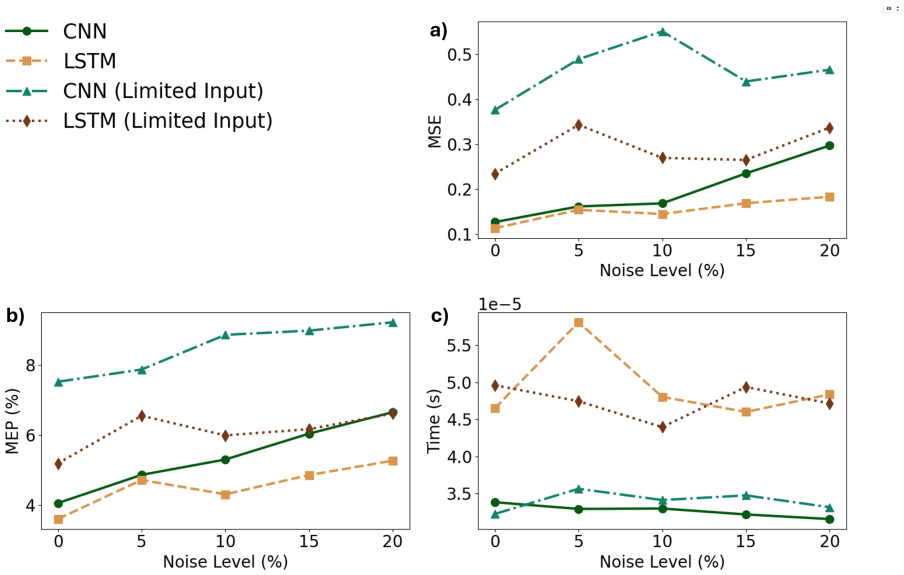

Figure 5: Impact of Noise Levels on the Performance of CNN and LSTM Models. a) Overall MSE: Depicts the Mean Squared Error for both CNN and LSTM models under standard and limited input conditions across varying noise levels, showing a consistent increase in MSE with higher noise for all configurations. b) MEP: Illustrates the percentage error at maximum for each model configuration across different noise levels, highlighting the sensitivity to noise, especially in the limited input scenarios. c) Average Prediction Time per Timestep: Shows the prediction time variability for each model as noise levels increase. The prediction times for both models are negligible compared to the 0.25-second prediction horizon, achieving near real-time prediction.

vironments where data integrity cannot be guaranteed. Conversely, the LSTM model exhibited a more gradual increase in MEP and MSE under increasing noise levels, with MEP reaching 5.263 at 20% noise. This demonstrates the LSTM's inherent resilience to noise, suggesting its suitability for applications where data quality may be inconsistent.

3.2. Model Performance Under Limited Input Conditions

In this part of the analysis, we examine the performance of the CNN and LSTM models when deprived of historical pitch rate data, a scenario that tests each model's ability to predict based solely on other available aerodynamic data. This setup mimics conditions where primary flight sensors might fail or be unavailable, pushing the models to rely on secondary input types for state prediction.

The exclusion of pitch rate data had a pronounced impact on the CNN model's performance. This configuration exhibited an overall increase in MSE, with the lowest value recorded at 0.3761, significantly higher than its performance with pitch data included. MEP also saw a notable increase, starting at 7.5198 and peaking at 9.2201 as noise levels were escalated to 20%. These metrics underscore the critical role that pitch rate data plays in the CNN model's ability to make

accurate predictions, highlighting its dependency on comprehensive input data for optimal performance. Prediction times remained relatively stable, suggesting that the absence of pitch rate data did not affect the computational speed significantly but did compromise accuracy and reliability.

Similarly, the LSTM model experienced degradation in performance when operating without pitch rate inputs. The initial MSE was 0.2343, which, although lower than that of the CNN, still represented a considerable increase compared to the LSTM configuration with pitch rate data. The MEP increased progressively with higher noise levels, indicating that while the LSTM is generally more resilient to missing data types, its performance is noticeably hindered under such constraints. However, it maintained a lower MEP compared to the CNN across all noise levels, reinforcing its robustness in less-than-ideal input conditions.

The comparative analysis between CNN and LSTM models highlights the LSTM's relative robustness and lower dependency on pitch rate data compared to the CNN. While both models show increased errors and reduced reliability without pitch rate inputs, the LSTM's performance drop is less severe, suggesting that it may still provide reasonable accuracy and reliability in scenarios where primary sensor data is compromised or incomplete. This makes the LSTM model particularly valuable for applications requiring robust performance in the face of sensor unreliability or data gaps.

4. Conclusion

This study presented a comprehensive framework for advanced machine learning models, specifically 1D Convolutional Neural Networks (CNN) and Long Short-Term Memory (LSTM) networks, in predicting the flight states of unmanned aerial vehicles (UAVs) based on aerodynamic data sensed from aircraft wings. The main focus was to assess the potential of distributed aerodynamic parameters in enhancing the predictiveness and reliability of flight control systems, which is a novel approach in the realm of aerospace engineering.

Both models achieved prediction times that underscore their potential for real-time applications, highlighting the practical viability of integrating these advanced machine learning techniques into operational aerospace systems. The LSTM model, in particular, showed a superior ability to handle longer historical input data, which translated into more accurate predictions. This model proved to be robust across a range of operational conditions, especially in scenarios where data was affected by noise, underscoring its potential utility in environments where data reliability may fluctuate. In contrast, the CNN model, while requiring lower computation time, showed higher sensitivity to noise and a tendency to overfit with increasing input sizes, suggesting its best use in scenarios where rapid processing is prioritized over robustness.

In scenarios where pitch rate measurements were missing and only aerodynamic data were used, both models demonstrated significant resilience, with the LSTM notably outperforming the CNN. This highlights the LSTM's ability to maintain more accurate and reliable predictions even when available data are constrained—a crucial advantage in real-world applications where sensor data may not always be complete or reliable. The CNN, though slightly less robust under these conditions, still offers valuable capabilities for rapid response and decision-making in critical situations.

Future work should focus on refining these models by exploring hybrid approaches that combine the strengths of CNNs and LSTMs, potentially leading to even greater efficiency and accuracy. Additionally, real-world testing and integration into live aerospace systems would provide valuable data to further validate and refine the predictive capabilities of these models.

References

BAE. British engineers have successfully completed a stratospheric flight trial of bae systems' high altitude pseudo satellite uncrewed aerial system - phasa-35, July 2023. URL https://www.baesystems.com/en/article/phasa-35--completes-first-successful-stratospheric-flight.

Bartosz Binias, Dariusz Myszor, Henryk Palus, and Krzysztof A Cyran. Prediction of pilot's reaction time based on eeg signals. *Frontiers in neuroinformatics*, 14:6, 2020.

Richard E Brown and M Roger Fedde. Airflow sensors in the avian wing. *Journal of experimental biology*, 179(1):13–30, 1993.

Xi Chen, Fotis Kopsaftopoulos, Qi Wu, He Ren, and Fu-Kuo Chang. Flight state identification of a self-sensing wing via an improved feature selection method and machine learning approaches. *Sensors*, 18(5):1379, 2018.

Xi Chen, Fotis Kopsaftopoulos, Qi Wu, He Ren, and Fu-Kuo Chang. A self-adaptive 1d convolutional neural network for flight-state identification. *Sensors*, 19(2):275, 2019.

Alfonso del Carre, Norberto Goizueta, Arturo Muñoz-Simón, and Rafael Palacios. SHARPy: A dynamic aeroelastic simulation toolbox for very flexible aircraft and wind turbines, May 2023. URL https://doi.org/10.5281/zenodo.7988519.

Yoshiro Hamada, Kenichi Saitoh, and Noboru Kobiki. Gust alleviation control using prior gust information: Wind tunnel test results. *IFAC-PapersOnLine*, 52(12):128–133, 2019.

Ahmed Khalil and Nicolas Fezans. Performance enhancement of gust load alleviation systems for flexible aircraft using h optimal control with preview. 01 2019. doi: 10.2514/6.2019-0822.

Fotios Kopsaftopoulos, Raphael Nardari, Yu-Hung Li, Pengchuan Wang, and Fu-Kuo Chang. Stochastic global identification of a bio-inspired self-sensing composite uav wing via wind tunnel experiments. In *Health Monitoring of Structural and Biological Systems 2016*, volume 9805, pages 446–460. SPIE, 2016.

Fotis Kopsaftopoulos, Raphael Nardari, Yu-Hung Li, and FK Chang. Experimental identification of structural dynamics and aeroelastic properties of a self-sensing smart composite wing. In *Proceedings of the 10th International Workshop on Structural Health Monitoring*, 2015.

Fotis Kopsaftopoulos, Raphael Nardari, Yu-Hung Li, and Fu-Kuo Chang. A stochastic global identification framework for aerospace structures operating under varying flight states. *Mechanical Systems and Signal Processing*, 98:425–447, 2018.

Chris Regan and Christine Jutte. Survey of applications of active control technology for gust alleviation and new challenges for lighter-weight aircraft. 04 2012.

Susanne Sterbing-D'Angelo, Mohit Chadha, Chen Chiu, Ben Falk, Wei Xian, Janna Barcelo, John M Zook, and Cynthia F Moss. Bat wing sensors support flight control. *Proceedings of the National Academy of Sciences*, 108(27):11291–11296, 2011.